Mausam, (1993), **44**, 4, 321-328

551.515.1 (267)

A diagnostic analysis of MONEX-1979 onset vortex over the Arabian Sea

KSHUDIRAM SAHA
27, B-Road, Maharani Bagh, New Delhi-110065
and
SURANJANA SAHA
Development Division, National Meteorological Center, Washington, D. C. (U.S.A.)

(Received 20 May 1992, Modified 17 March 1993)

सार–मॉनेक्स-1979 के, अरब सागर के आंकड़ों के आधार पर, इस शोध-पत्र में एक भ्रामिल की संरचना, विकास और गति का विश्लेषण किया गया है। यह भ्रामिल, केरल तट के समीप, मानसून के अभ्युदय के दौरान लगभग जून के मध्य में बना और समुद्र के बीच चक्रवाती तूफान में विकसित हो गया तथा ओमान के तट की ओर बढ़ते हुए समाप्त हो गया। उष्मा अभिकलनों से चक्रवात के विभिन्न चतुर्थांशों का विभेदक आचरण स्पष्ट होता है। इन अभिकलनों ने उत्तर-पश्चिमी व अन्य चतुर्थांशों के मध्य डायबेटिक उष्मण, स्थानीय तापमान प्रवृत्ति, तापीय अभिवहन और रुद्धोष्म उष्मण अथवा शीतलन के ऊर्ध्वाधर बंटन से सम्बन्धित विभिन्न लक्षणों को स्पष्ट किया है। इस अध्ययन से उपरोक्त भ्रामिल के साथ पश्चिम दिशा की ओर गतिशील दो उपोष्णीय पश्चिमी द्रोणियों के टकराव का पता चला है जिन्होंने संभवतः उष्ण (शीतल) अभिवहन के माध्यम से इस भ्रामिल के विस्फोटक विकास में मदद की। ऐसा प्रतीत होता है कि ऊर्जा के बैरोट्रोपिक और बैरोक्लिनिक दोनों प्रकार के परिवर्तनों में चक्रवात को आवश्यक ऊर्जा प्रदान की, यद्यपि विकास की विभिन्न दशाओं और भिन्न ऊंचाईयों पर एक प्रकार की ऊर्जा का दूसरी प्रकार की ऊर्जा पर वर्चस्व बना रहा। ऐसा लगता है कि संघनन उष्मा ने भी चक्रवात को विकसित करने में मदद की।

ABSTRACT. Based on MONEX-1979 data over the Arabian Sea, the paper analyses observationally the structure, development and movement of a vortex which formed during onset of the monsoon around mid-June near the coast of Kerala, developed into a cyclonic storm at mid-sea and moved towards the coast of Oman to die out there. Heat budget computations bring out the differential behaviour of the different quadrants of the disturbance and appear to highlight the contrasting features between the northwestern and the other quadrants in regard to vertical distributions of diabatic heating, local temperature tendency, thermal advection and adiabatic heating or cooling. The study reveals an interaction of the vortex with two eastward-propagating sub-tropical westerly troughs which might have contributed significantly to its explosive development (decay) through warm (cold) advection. Both barotropic and baroclinic energy conversions appear to supply energy to the storm, though there appears to be a dominance of one over the other at different stages of development and at different heights. It seems likely that condensation heating also contributed to development of the storm.

Key words — Monsoon onset, Onset vortex, MONEX-1979, Arabian Sea vortex.

1. Introduction

In June 1979, when the Summer Monsoon Experiment (SMONEX) was in progress over the Arabian Sea, a vortex formed at the leading edge of the advancing strong westerly monsoon current and was centred msl near the Lakshadweep islands on 15 June (depression at estimated central pressure 1000 hPa). Moving initially north/northwestward and later almost westward, it developed into a deep depression/cyclonic storm reaching peak intensity at mid-sea on 18 June (estimated central pressure 993 hPa) as it headed towards the coast of Oman and weakened rapidly after landfall on 20 June.

Several studies (*e.g.*, Krishnamurti *et al.* 1981, Mak and Kao 1982) analysed the dynamical instability of the flow associated with this vortex and concluded that barotropic energy conversion arising from strong horizontal shear of the zonal wind might have been the dominant process in the initiation of the disturbance. Ramanathan (1981) who used a multi-level primitive equation model concluded that while the barotropic processes were dominant in lower tropospheric levels, baroclinic processes in the upper levels were responsible for the further growth of the disturbance into a depression. A number of studies (*e.g.*, Mak 1982) have emphasized the possible role of moist convection in the initiation of the vortex.

Unfortunately, as remarked by Mak (1987), a detailed diagnostic analysis of this spectacular storm has not yet been reported in literature. The reasons for this are not known. There are several aspects of this storm

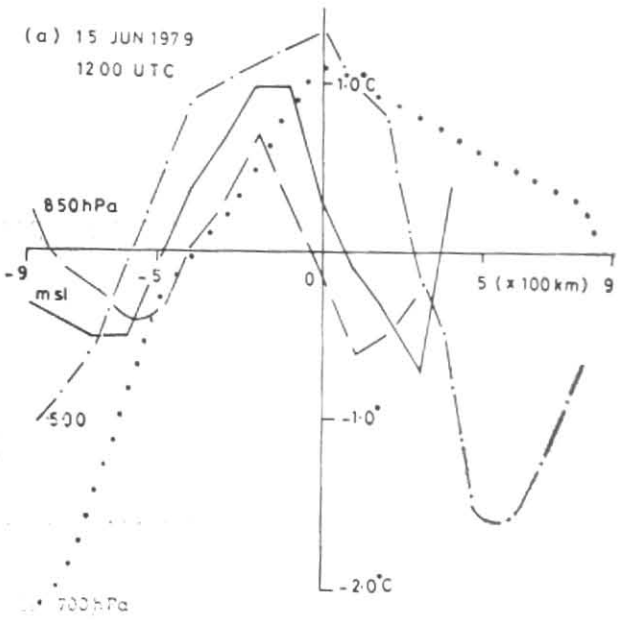

Fig. 1(a). Longitudinal distribution of zonal temperature anomaly (C) (deviation from zonal mean temperature) relative to the vortex centre on 15 June at msl, 850, 700 and 500 hPa

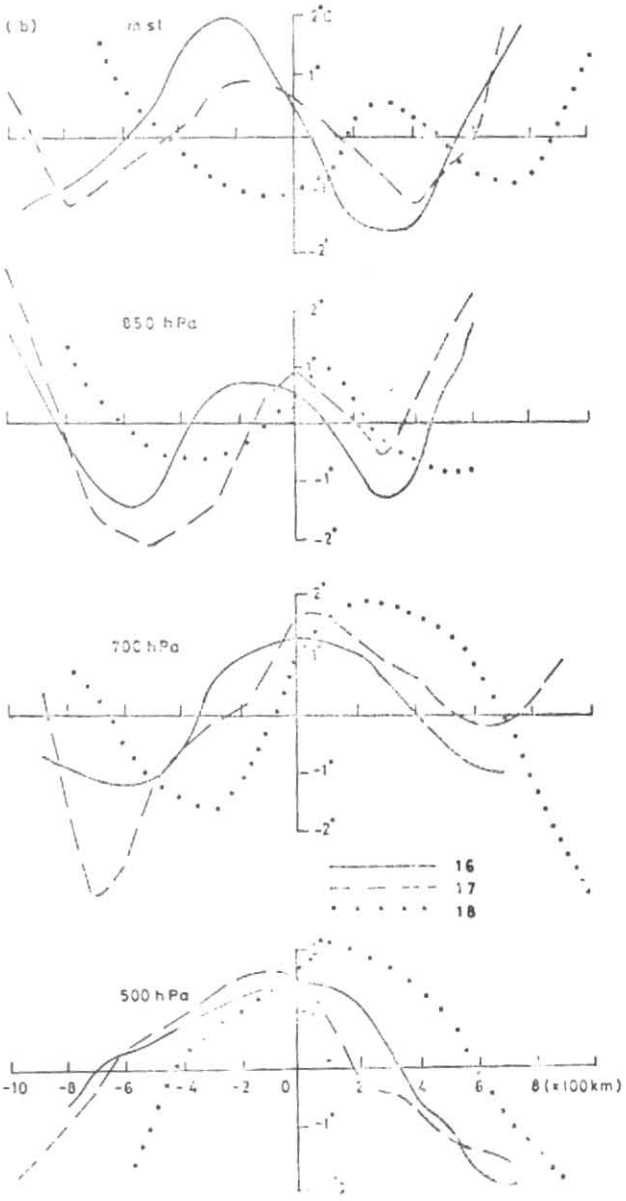

Fig. 1(b). Longitudinal distribution of zonal temperature anomaly (C) (deviation from zonal mean temperature) relative to vortex centre at msl, 850, 700 and 500 hPa on 16, 17 and 18 June

including its structure and development which have remained rather obscure, even though the SMONEX was carried out nearly a decade and a half ago. Clearly, further studies are required to elucidate some of the problems. The present investigation may be said to be an attempt in this direction. In section 2, we describe data and analysis. The wave structure of the vortex as it appears in flow and thermal fields at isobaric surfaces is described in section 3. Results of computation of a heat budget which may help in understanding the physical processes within the vortex circulation such as diabatic and adiabatic heating and cooling are presented in section 4. The vortex during its lifetime interacted with at least two eastward-propagating sub-tropical disturbances. Some aspects of this interaction believed to be involved in the development and movement of the vortex are discussed in section 5. Some aspects of energetics and energy conversions are discussed in section 6. Section 7 summarizes the main findings.

2. Data and analysis

Basic data for the study comprise daily 12 UTC winds and temperatures at msl and standard pressure surfaces 850, 700, 500, 300 and 200 hPa over domain, 0-40° N, 50-100° E, during period 15 through 18 June 1979. Data sources include the conventional synoptic maps of the India Meteorological Department (IMD) and the following special publications of the International MONEX Management Centre (IMMC) available with the IMD Headquarters at New Delhi :

FGGE MONEX Datasets :

No. 1.4. Ships data (FGGE ships)—Upper wind data,

No. 2.1. Aircraft data — Dropwindsondes,

No. 2.3. Aircraft data (flight level) — AVRO,

No. 2.4. Aircraft data — Dropwindsonde wind data, and

No. 4.1. Land station data — Upper air observations.

Supplementary wind data from special observing platforms were obtained from an atlas published by Krishnamurti *et al.* (1979). Information regarding large-scale cloud distributions associated with the vortex was also obtained from the same source.

The coverage, quality and reliability of the datasets used, which were obtained from so many diverse platforms, leave much to be desired, though they wet-

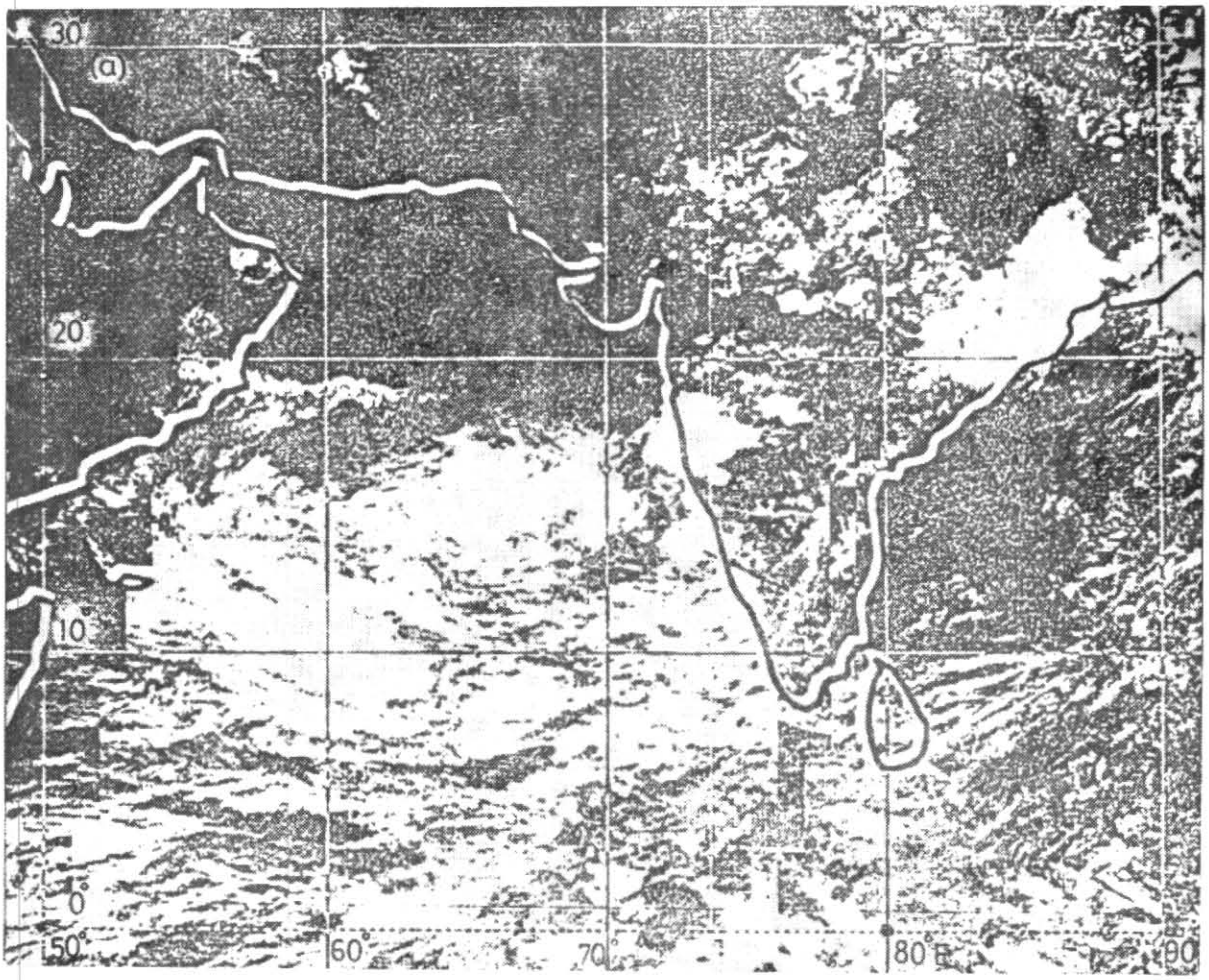

Fig. 2(a). Daily cloud distributions over the Arabian Sea during 15 June 1979

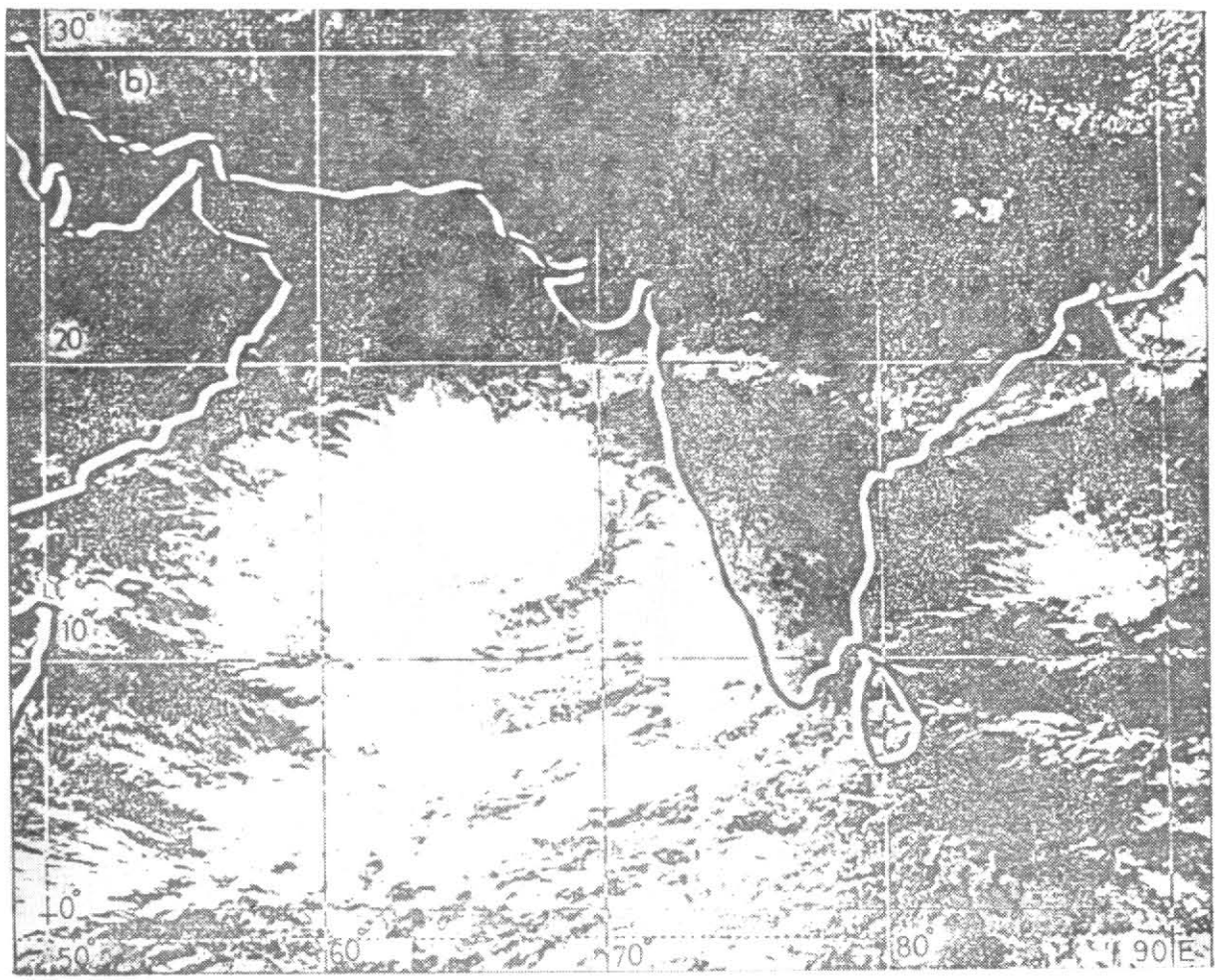

Fig. 2(b). Daily cloud distributions over the Arabian Sea during 16 June 1979

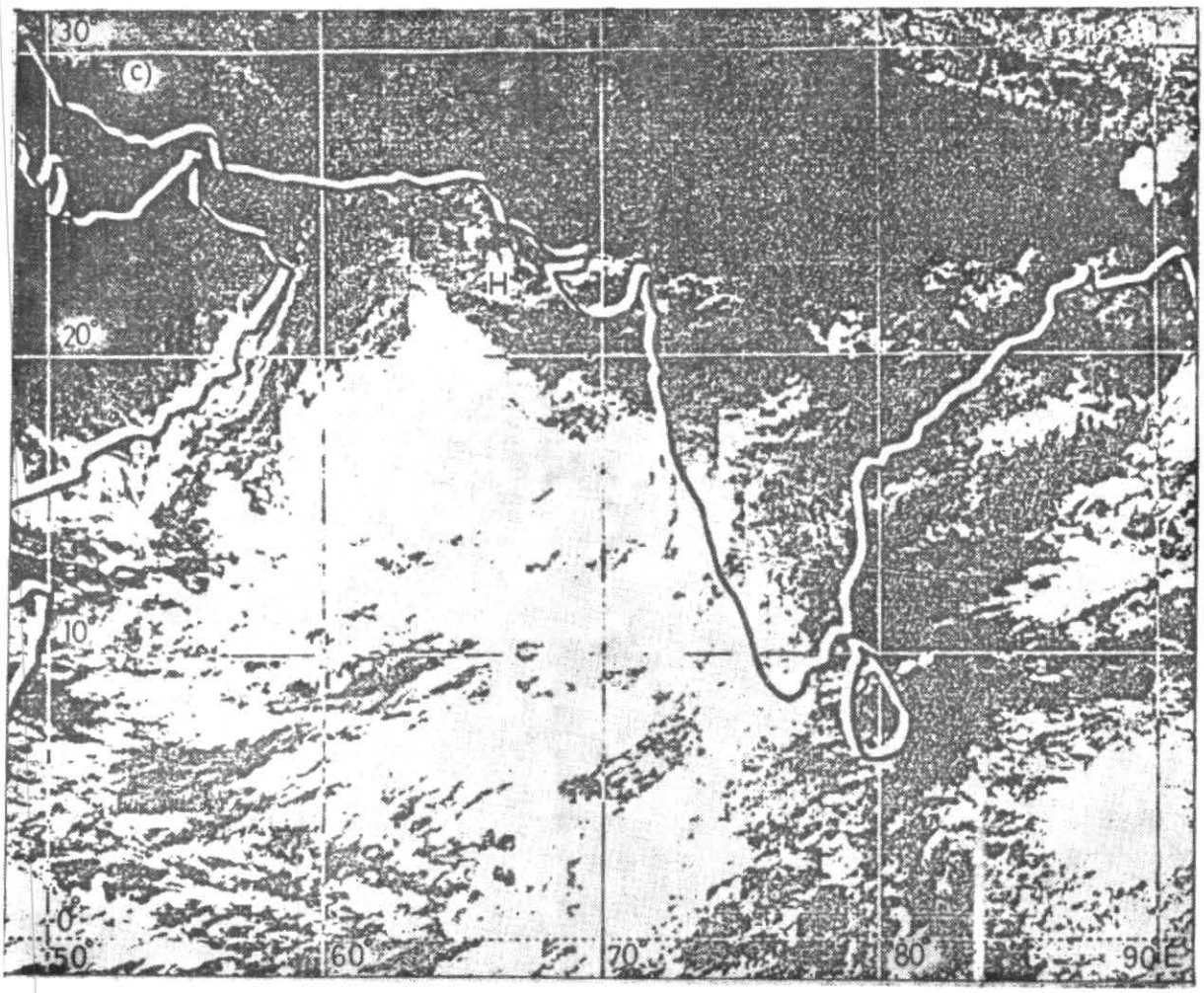

Fig. 2(c). Daily cloud distributions over the Arabian Sea during 17 June 1979

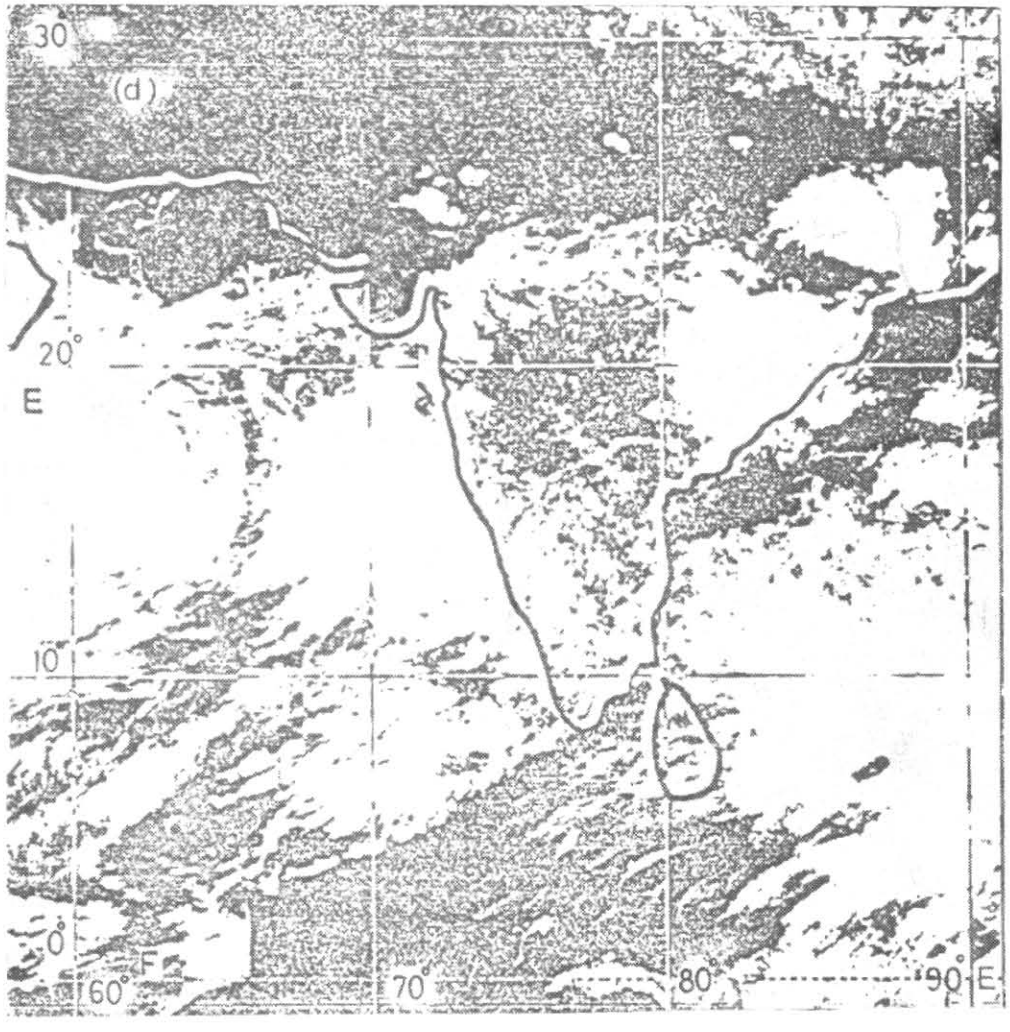

Fig. 2(d). Daily cloud distributions over the Arabian Sea during 18 June 1979

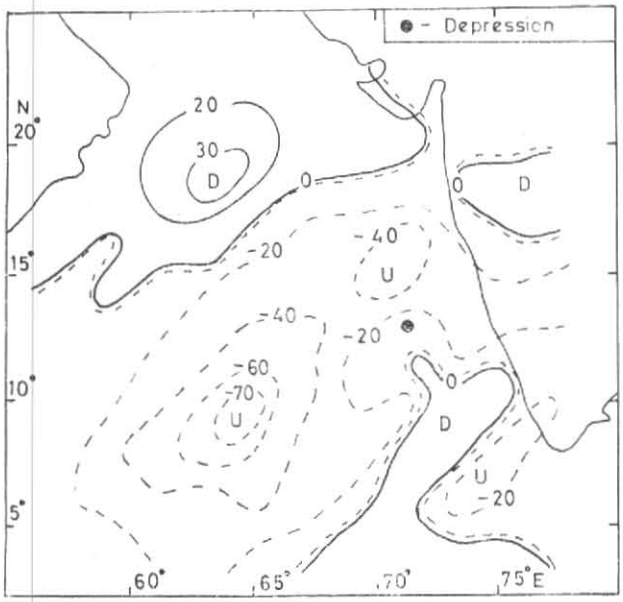

Fig. 3. Distribution of vertical velocity (unit : 10^{-4} hPa s^{-1}) at 500 hPa on 15 June. Negative (positive) values denote upward (downward) motion. U—upward, D—downward

decidedly the best so far that one could aspire to get on a usually-data-void ocean. Data coverage was generally poor over the western part of the Arabian Sea but fairly satisfactory over the eastern part. Barring a few exceptions, wind and temperature data were fairly reliable over a major part of the sea. Gupta *et al.* (1980) who carried out an intercomparison of wind and temperature data obtained from different observing platforms conclude, inter alia, that wind direction and speed obtained from satellite-derived cloud motion vectors agree well with other data when the wind speed was less than 25 m/s and that dry-bulb temperature difference between ship and dropwindsonde data was generally within +1.5° C and —1.5° C.

The available wind and temperature data were analysed to determine some of the characteristics of the flow and thermal fields associated with the vortex. The horizontal temperature distribution suggested an easterly thermal wind over the region practically at all heights of the troposphere. The resulting analysis was used to find out the horizontal and vertical structure of the vortex, work out a heat budget and compute energy conversions. The analysis was also used to study a case of interaction of the vortex with travelling disturbances of the sub-tropical belt.

An examination of large-scale cloud distributions over the Arabian Sea, reproduced in Figs. 2 (a–d), reveals the presence of two distinct cloud groups. One of these which extended along the west coast of India and over adjoining sea areas appeared to be related to low-level convergence and orography and lay to the east of the vortex centre. The other group which appeared to be directly associated with the vortex circulation lay to the west of the centre. As the vortex moved away westward, the first group which was associated with monsoon onset extended northward along the coast and also covered a wider area of the neighbouring sea.

3. Structure

The vortex reveals a wave structure with well-defined warm and cold sectors in the east-west direction drawn through its circulation centre at pressure surfaces below 500 hPa. This is evident from Fig. 1(a) which shows the longitudinal distribution of zonal temperature anomaly (deviation from zonal mean temperature) relative to the circulation centre at msl, 850, 700 and 500 hPa on 15 June and from Fig. 1(b) which shows the zonal temperature anomaly on 16, 17 and 18 June at different pressure surfaces. Together, they seem to bring out the following structural characteristics:

(*i*) The vortex appears to have an M-shaped thermal structure with a warm sector lying between two cold sectors in east-west direction.

(*ii*) The wave-length of the vortex appears to be in the range 1000-1500 km at msl and 850 hPa and about 1500-2000 km at 700 and 500 hPa. The temperature amplitude is about 1 to 2°C at all levels.

(*iii*) A phase difference between the wind and the temperature fields appears to stand out in our analysis and undergo change with time and height as shown in Table 1 (a phase difference is taken as positive or negative according as the warmest temperature anomaly lies to the west or east of the circulation centre and as zero when the warmest anomaly coincides with the centre).

A phase difference of the kind reported in Table 1 was first reported by Saha and Chang (1983) in the case of a developing monsoon depression over the Bay of Bengal. In the present case, it is likely that a positive phase difference at msl and 850 hPa on 15, 16 and 17 June suggests a developing stage of the vortex. A negative phase difference at all levels on 18 June may signify the beginning of a dissipating stage.

4. Heat budget

Large-scale convective clouds to the west of the vortex centre especially over the southwestern quadrant

TABLE 1

Phase difference between wind and temperature fields associated with the onset vortex at msl and different pressure surfaces (a phase difference is taken as positive or negative according as the warmest temperature anomaly lies to the west or east of the circulation centre and as zero when the two coincide)

Pressure surface (hPa)	Date (June)			
	15	16	17	18
msl	$\pi/3$	$2\pi/5$	$4\pi/15$	$-2\pi/5$
850	$\pi/3$	$4\pi/5$	0	$-2\pi/15$
700	0	0	$-\pi/15$	$-\pi/3$
500	0	0	$\pi/15$	$-2\pi/15$

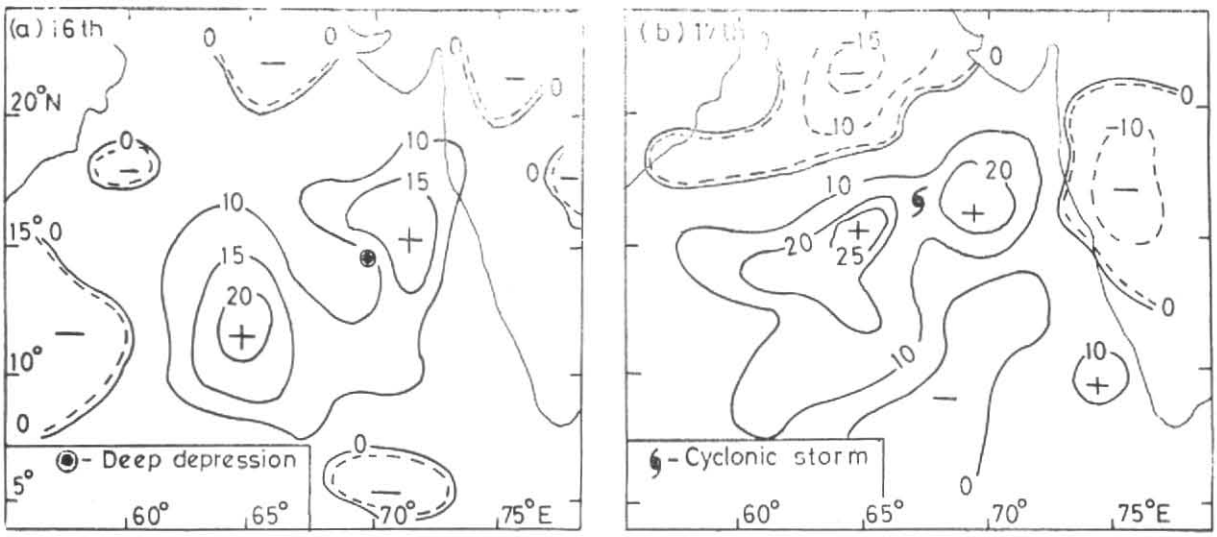

Figs. 4 (a & b). Horizontal distribution of vertically integrated diabatic heating (unit : 10^2 W m^{-2}) on : (a) 16, and (b) 17 June

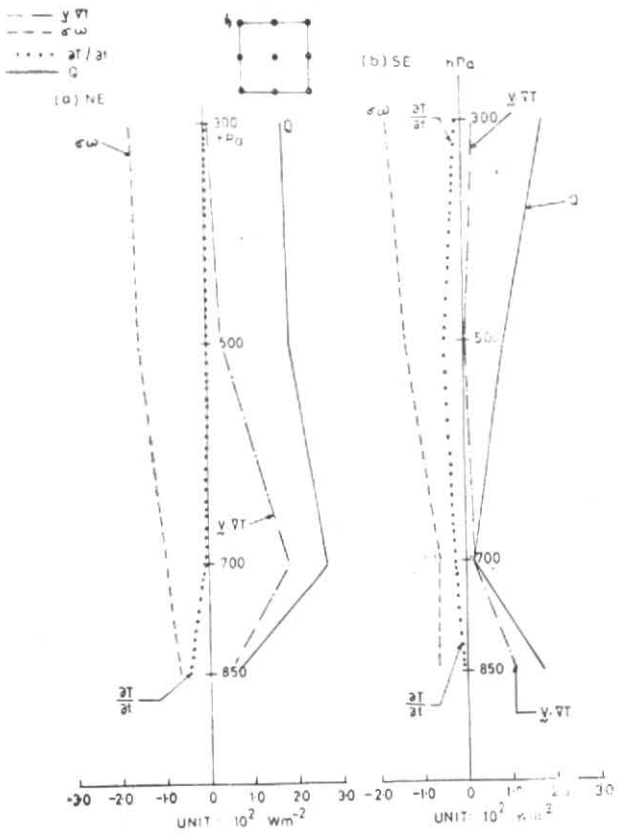

Figs. 5 (a & b). Vertical distribution of horizontally-averaged values of the terms of the heat budget equation on 17 June in different quadrants of the vortex : (a) NE, and (b) SE. Values are averaged over a 9-point grid indicated in the respective diagrams

of the vortex suggest considerable release of latent heat over that area. However, a direct measure of this diabatic heating as well as that arising from radiation and sensible heat flux across boundaries is difficult to obtain in the absence of adequate data. In this circumstances, we computed diabatic heating indirectly from the first law of thermodynamics in the form :

$$Q = \left(c_p/g\right)\int\left(\frac{\partial T}{\partial t} + \mathbf{V}.\ \nabla T - \sigma\omega\right)\delta p$$

where, Q—The rate of diabatic heating,

c_p—Specific heat of air at constant pressure p,

g—Acceleration due to gravity,

T—Air temperature in degrees Kelvin,

$\mathbf{V}$—Wind vector (with components u,v along x, y axes respectively),

ω—Vertical p-velocity,

σ—Static stability parameter $\left(= \frac{RT}{pc_p} - \frac{\partial T}{\partial p}\right)$, and

R— Gas constant for air.

In the heat budget equation, the right-hand side constitutes the adiabatic response of the atmosphere to the diabatic heating or cooling and the three terms represent respectively the local heating or cooling tendency, horizontal thermal advection and adiabatic heating or cooling due to vertical motion. These terms were evaluated at the standard pressure surfaces 850, 700, 500 and 300 hPa using a 2 degree latitude-longitude grid and a centred finite-differencing scheme in both space and time. Since we had data for 4 days, temperature tendency could be calculated for 16 and 17 June only. Vertical p-velocity was computed using the continuity equation in which the layer-mean horizontal wind divergence was integrated in the vertical from 925 hPa to 250 hPa using the lower boundary condition, $\omega_s = \mathbf{V}_s \cdot \nabla p_s$, where, ω_s is vertical velocity at surface pressure p_s. The well-known

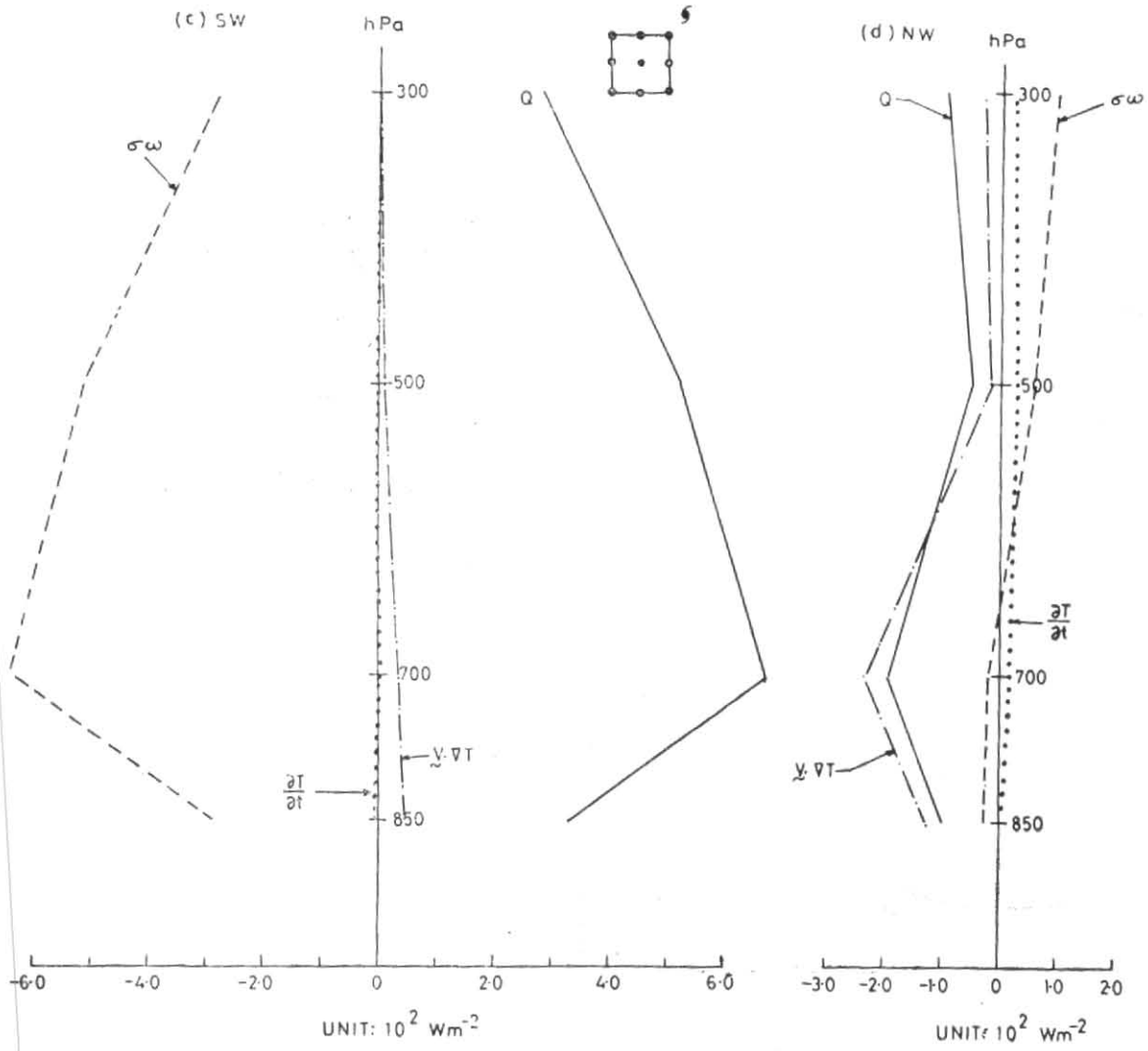

Figs. 5(c & d). Vertical distribution of horizontally-averaged values of the terms of the heat budget equation on 17 June in different quadrants of the vortex : (c) SW, and (d) NW quadrant. Values are averaged over a 9-point grid indicated in the respective diagrams

TABLES 2(a&b)

Kinetic energy of total flow and vortex circulation in different pressure layers [values are averaged over a 9×9 grid-point network centred at the vortex centre (unit : 10^5 Jm^{-2})]

Date	Pressure layers (hPa)				Whole layer
	925-775	775-600	600-400	400-250	925-250
	(a) Total flow				
15	0.94	1.26	0.59	0.29	3.10
16	1.49	1.35	0.54	0.25	3.64
17	2.44	2.53	1.20	0.54	6.72
18	3.05	2.00	2.19	0.77	8.01
	(b) Vortex circulation				
15	0.3	0.4	0.3	0.2	1.1
16	0.3	0.2	0.2	0.1	0.8
17	0.4	0.6	0.5	0.4	1.9
18	0.7	0.6	1.0	0.3	2.6

O'Brien correction was applied to the computed vertical velocity at the different pressure surfaces so as to force the magnitude of the vertical velocity at the top to zero. It was noted that the correction did not materially alter the direction and magnitude of the vertical velocity computed by the continuity equation. Since divergence calculated from observed wind is often subject to large errors and its vertical integration fails to achieve adequate mass compensation to explain observed small pressure tendency at the lower boundary, the use of continuity equation to compute vertical motion using observed wind as input has been viewed with skepticism in the past (*e.g.*, Ramage 1971). However, in the present study, we were encouraged by a large measure of consistency between the analysed wind and temperature fields and a qualitative agreement between the computed vertical motion field and the distributions of large-scale clouding and precipitation. Fig. 3 presents an example of the computed vertical motion field at 500 hPa at 12 UTC on 15 June 1979. The distribution of total diabatic heating, vertically-integrated between 925 and 250 hPa, on 16 and 17

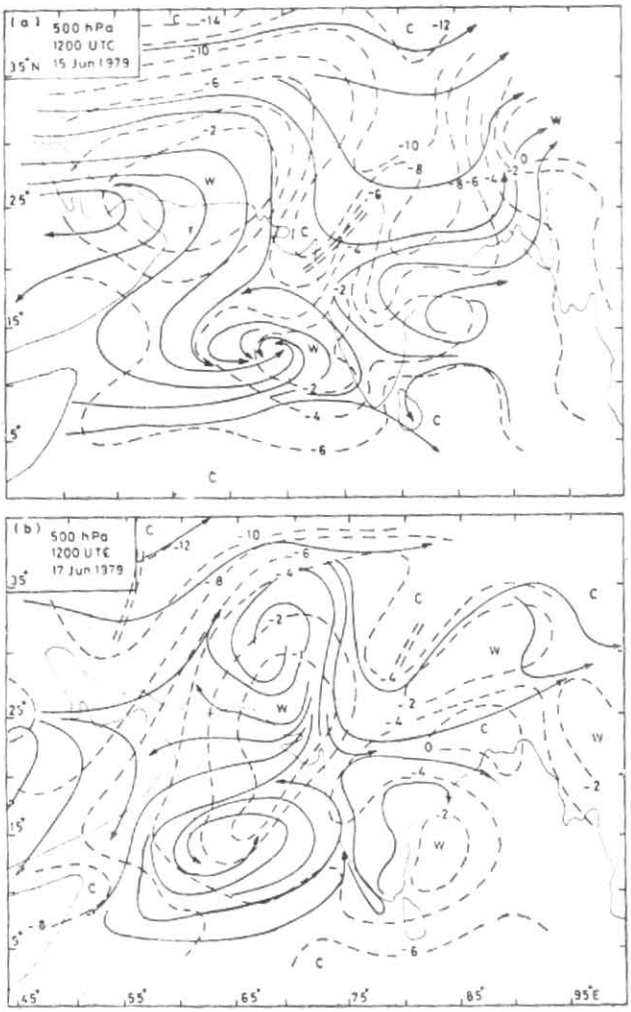

Figs. 6 (a & b). Synoptic situation showing streamlines and isotherms at 500 hPa at 12 UTC on : (a) 15 June, and (b) 17 June

June, is presented in Figs. 4 (a & b) respectively. It shows large positive values in areas of strong penetrative convection to both west and east of the vortex centre, representing respectively the cloud group associated with the mid-ocean onset vortex and that associated with the regular monsoon onset along the west coast of India. Negative values appear at some distance to the northwest and the southeast of the centre, where besides areas of penetrative convection some cloud-free areas also appear. In Figs. 5 (a-d), we show the vertical distribution of the values of the different terms of the heat budget equation over the four quadrants of the vortex (values are averaged over a nine-point grid in the respective quadrant relative to the vortex centre, as shown in the diagrams) and the results would seem to bring out the following salient feature :

(*i*) *Northeast quadrant* [Fig. 5 (a)]

Diabatic heating is positive throughout the troposphere. It appears to be compensated by cold advection and penetrative convection. There is considerable local cooling in the lower troposphere (below 700 hPa), with little temperature tendency aloft.

(*ii*) *Southeast quadrant* [Fig. 5(b)]

Diabatic heating is positive at all heights though it reaches a small value at 700 hPa. As over the northeast quadrant, it is compensated by cold advection, mostly in the lower troposphere (below 700 hPa) and also by some penetrative convection. The local temperature tendency is negative throughout the troposphere.

(*iii*) *Southwest quadrant* [(Fig. 5(c)]

Diabatic heating reaches high positive values throughout the troposphere with a maximum (674.7 W m^{-2}) at about 700 hPa. Most of this heating is compensated by adiabatic cooling in large-scale strong penetrative convection. There is some cold advection below about 500 hPa. Local temperature tendency is almost negligible.

(*iv*) *Northwest quadrant* [(Fig. 5(d)]

The vertical distribution of the different heat budget terms here appears to be very different from those over the other quadrants. Diabatic heating turns out to be negative throughout the troposphere. There is strong warm advection especially in the lower troposphere below about 500 hPa. Some adiabatic cooling appears at the lower levels (below about 650 hPa) but subsidence warming prevails aloft. Local temperature tendency appears to be strongly positive throughout the troposphere. Possible significance of this strong warming of the atmosphere in the context of development of the vortex will be discussed in the section that follows.

5. Interaction with sub-tropical disturbances

In our search for a plausible physical explanation for the dramatic development and change in direction of movement of the vortex after 16 June, we examined the daily synoptic maps and found that there was evidence of interaction of the vortex with at least two distinct sub-tropical westerly troughs during its lifetime. During the interaction with the first westerly trough, a typical example of which is presented in Fig. 6 (a) which shows the flow pattern and isotherms at 500 hPa at 12 UTC on 15 June, warm advection from the north to the west of the vortex centre was restricted somewhat by the presence of the cold sector of the deep westerly trough over the northeastern corner of the Arabian Sea. It seems likely that subdued development and a north/northwestward movement of the vortex were forced by interaction with this westerly trough. The situation, however, changed dramatically after 16 June. The cold sector of the first westerly trough moved away eastward making room for the warm sector of a second westerly trough advancing from the west. Fig. 6(b) which presents the synoptic situation at 500 hPa at 12 UTC on 17 June shows the vortex in the grip of this new westerly trough with their warm sectors well locked up with each other. The coupling causes strong warm advection from the north to the west of the vortex centre [(Fig. 5(d)]. We are thus led to believe that it is this warm advection which might have contributed significantly to the explosive development of the vortex.

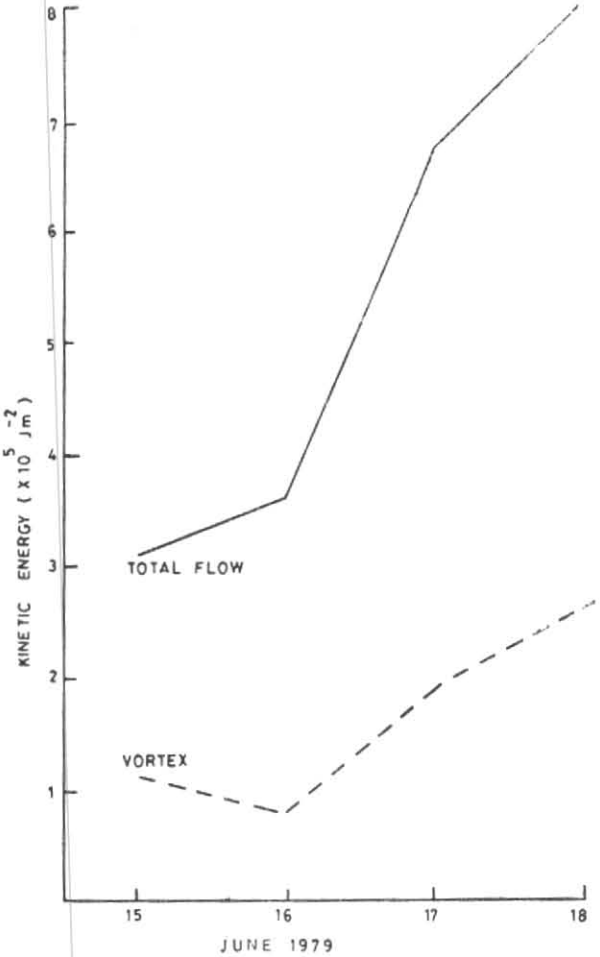

Fig. 7. Evolution of kinetic energy of the total flow and the vortex circulation from 15 through 18 June. Values are vertically integrated and horizontally averaged (unit : 10^5 J m^{-2})

As mentioned earlier, the vortex after attaining peak intensity on or about 18 June gradually weakened and died within 2 or 3 days. What brought about this change in the intensity of the vortex ? An examination of the synoptic maps suggests that warm advection to the west of the vortex centre which is essential for its maintenance decreases after 18 June as the two disturbances move in opposite directions and the vortex encounters increasing cold advection from the cold sector of the westerly trough over the northwestern corner of the Arabian Sea.

6. Energy for development

The dramatic development of the vortex from 16 to 18 June is well reflected in the change of its kinetic energy presented in Fig. 7 which shows the daily values of the kinetic energy of the total flow and the vortex circulation, averaged over a 9×9 grid-point network centred at the vortex centre and integrated from 925 to 250 hPa. The values of kinetic energy of the circulations in different pressure layers are presented in Tables 2 (a&b) for the total flow and the vortex circulation respectively.

TABLES 3(a & b)

Barotropic and baroclinic energy conversions in different pressure layers [values are averaged over a 9 × 9 grid-point network centred at the vortex centre (unit : 10^{-2} Wm^{-2})]

Date	Pressure layer (hPa) 925-775	775-600	600-400	400-250	Whole layer 925-250
	(a) Barotropic energy conversion				
15	19.9	33.6	7.6	−.32	57.9
16	−15.3	−8.1	−9.5	−1.2	−34.1
17	−19.6	165.5	34.0	−2.8	177.1
18	11.8	36.9	86.5	8.5	143.6
	(b) Baroclinic energy conversion				
15	2.5	−12.4	−57.3	7.1	−60.2
16	−13.5	31.8	55.3	81.8	155.4
17	−48.1	−10.2	98.6	40.2	80.6
18	2.1	−119.5	20.0	−17.8	−115.2

The question as to where the vortex got its energy from may be well debated. It is not suggested that the only source of energy for its development came from the thermal advection from an external source as described in the foregoing section, though it might well have triggered off the development process. Since the flow had strong horizontal and vertical shear and there was widespread convection in the field of the vortex, it seems likely that other energy sources such as barotropic and baroclinic energy conversions and condensation heating were also involved. In the past, the relative importance of these various processes for the growth and maintenance of a tropical disturbance has been very much under study but the problem still remains. In the present study, we computed barotropic and baroclinic energy conversions using the formulations (Lorenz 1967):

Barotropic energy conversion

$$\left\langle \bar{K}.K' \right\rangle = -\left(1/g\right)\int\left\{\left[u'v'\right]\frac{\partial}{\partial y}\left[u\right] + \left[u'\omega'\right]\frac{\partial}{\partial p}\left[u\right] + \left[v'v'\right]\frac{\partial}{\partial y}\left[v\right] + \left[v'\omega'\right]\frac{\partial}{\partial p}\left[v\right]\right\}\delta p$$

Baroclinic energy conversion

$$\left\langle P'.K' \right\rangle = -\left(R/g\right)\int\left(\left[\omega'T'\right]/p\right)\delta p$$

where, $\bar{K}$, K' and P' are zonal mean kinetic energy, eddy kinetic energy and eddy available potential energy respectively over a closed domain, the prime denotes a deviation from zonal average [ ] and the two terms within the angular brackets denote conversion from the first to the second and the other terms have their usual meanings.

Results of our computations with values averaged over a 9×9 grid-point network centred at the vortex centre are presented in Tables 3(a&b) for barotropic and baroclinic energy conversions respectively and appear to be revealing. On 15 June, the barotropic process appears to dominate, with only a slight contribution from the baroclinic process at low and high levels. The situation appears to change markedly on 16 June when the vortex starts developing. Barotropic energy conversion is

negative throughout the troposphere whereas baroclinic energy conversion is very strongly positive in all the vertical layers except the lowest below 775 hPa. However, on 17 June, the barotropic and the baroclinic processes are both strongly positive, the former between 775 and 400 hPa and the latter between 600 and 250 hPa. On 18 June, the barotropic process dominates again, while the baroclinic process weakens.

Current thinking emphasizes the role of moist convection in the development and maintenance of tropical disturbances (*e.g.*, Mak 1982). There is evidence of strong penetrative convection to the west of the vortex centre, especially over the southwestern quadrant of the vortex, after its development on 16 June and it seems likely that through a co-operative mechanism between the convective clouds and the vortex, generally known as the conditional instability of the second kind (CISK), convective heating made a significant contribution to the development of the vortex.

We are thus led to conclude that while barotropic, baroclinic and condensation processes might all have made their respective contributions to the formation and maintenance of the vortex, its explosive development and subsequent decay were in all probability triggered by its interaction with a baroclinic disturbance in the sub-tropical westerlies.

7. Summary

The findings of the present study may be summarized as follows :

(*i*) The vortex has a baroclinic structure with well defined warm and cold sectors in the east-west direction through its circulation centre.

(*ii*) A phase difference appears to exist between the wind and the temperature fields in the lower troposphere which changes with height and stage of development. A phase difference is regarded as positive when the warmest zonal anomaly lies to the west of the circulation centre. A positive phase difference appears to be a characteristic feature of a developing vortex.

(*iii*) Heat budget computations bring out the differential behaviour of the different quadrants of the disturbance and appear to highlight the contrasting features between the northwestern quadrant and the other quadrants in regard to diabatic heating, heating and cooling.

(*iv*) The vortex appears to derive its energy from both barotropic and baroclinic energy conversion processes, though some degree of complementarity appears to exist between the two. When the vortex is fully developed, energy conversions from both the processes are well in evidence. Condensation heating also appears to contribute to development of the disturbance.

(*v*) Development of the vortex appears to have been triggered off by its coupling with the warm sector of an eastward-propagating sub-tropical westerly trough which caused large-scale warm advection from the north to the west of the vortex centre. The vortex decayed when the coupling ended and cold advection replaced warm advection. The mechanism appears to be similar to that found by Saha and Chang (1983) in respect of monsoon depressions over the Bay of Bengal.

Acknowledgements

The authors' grateful thanks are due to the Director General of Meteorology, India Meteorological Department, New Delhi and the Director, Indian Institute of Tropical Meteorology, Pune, for facilities extended during preparation of the paper. They are grateful to Dr. H.M. Van Den Dool, National Meteorological Center, U.S.A. and an anonymous reviewer for their helpful comments on a first draft of the paper.

References

Gupta, M.G., Pant, M.C. and Rawat, M.S., 1980, Intercomparison of temperature data obtained from different observing systems during MONEX, FGGE Operations Rep., **9 (Pt B)**, 1-335.

Krishnamurti, T.N., Ardanuy, P., Ramanathan, Y. and Pasch, R., 1979, "Quick Look Summer MONEX Atlas-Part II: The onset phase", Rep. No. 79-5, Dept. of Meteorology, Florida State Univ., Tallahassee, Fla, U.S.A., 1-205.

Krishnamurti, T.N., Ardanuy, P., Ramanathan, Y. and Pasch, R., 1981, "On the onset vortex of the summer monsoons, *Mon. Weath. Rev.*, **109**, 344-363.

Lorenz, E.N., 1967, The nature and theory of the general circulation of the atmosphere, World Meteorological Organisation, 1-161.

Mak, M. and Kao, J.C.Y., 1982, "An instability study of the onset-vortex of the southwest monsoon", 1979, *Tellus*, **34**, 358-368.

Mak, M., 1982, "On moist quasi-geostrophic baroclinic instability", *J. Atmos. Sci.*, **39**, 2028-2037.

Mak, M., 1987, Synoptic scale disturbances in the summer monsoon, Monsoon Meteorology (Ed: Chang and Krishnamurti), Oxford Univ. Press, 1-544.

Ramage, C.S., 1971, Monsoon Meteorology, Academic Press, 297 pp.

Ramanathan, Y., 1981, "Onset of monsoon in the Arabian Sea during 1979, Int. Conf. on early results of FGGE and large-scale aspects of its monsoon expts (condensed papers and meeting report), Tallahassee, Fla, U.S.A., 13-34.

Saha, K.R. and Chang, C.P., 1983, "The baroclinic processes of monsoon depressions, *Mon. Weath. Rev.*, **111**, 1506-1514.